Characterization of the western Caribbean Sea waters through *in vivo* chlorophyll fluorescence

Caracterización de las aguas del Mar Caribe occidental mediante clorofila por fluorescencia *in vivo*

Raúl Aguirre Gómez[1*] *& Olivia Salmerón García*[1]

ABSTRACT
This paper presents the characteristics of fluorescence for the Caribbean Sea. Hydrographic and fluorometric data were gathered at the upper mixed layer during an oceanographic campaign carried out in the summer of 2001, from the Yucatan Peninsula to Colombian waters. *In vivo* fluorescence profiles show a conspicuous subsurface chlorophyll maximum located at a depth of around 107 m. These profiles are characteristic of oligotrophic waters such as those of the western Caribbean Sea.

Keywords: *In vivo* Fluorescence, Caribbean Sea, hydrographic measurements, upper mixed layer, subsurface chlorophyll maximum.

RESUMEN
En este artículo se presentan las características de fluorescencia del Mar Caribe. Se recolectaron datos hidrográficos y fluorométricos en la capa superior de mezcla durante una campaña oceanográfica realizada el verano de 2001, desde la península de Yucatán hasta aguas colombianas. Los perfiles de fluorescencia *in vivo* muestran un máximo subsuperficial de clorofila localizado alrededor de los 107 m de profundidad. Estos perfiles son característicos de aguas oligotróficas como las del Mar Caribe occidental.

Palabras claves: Fluorescencia *in vivo*, Mar Caribe, mediciones hidrográficas, capa superior de mezcla, máximo subsuperficial de clorofila.

INTRODUCTION

The Caribbean Sea is the largest adjacent sea of the Atlantic Ocean. It has an upper mixed layer of about 50 m, which quickly responds to atmospheric forcing. Circulation at this layer is mainly controlled by the Caribbean Current. The physical characteristics of the Caribbean Sea have been approached from different perspectives in other studies (*e.g.,* Gordon, 1967; Etter *et al.* 1987; Kinder *et al*. 1985; Müller-Karger *et al*. 1989; Gallegos, 1996; Gallegos & Czitrom, 1997; Sheinbaum *et al*. 1997; Sheng & Tang, 2003).

Conservative properties of the Caribbean Sea such as temperature and salinity, represented as water mass, remained approximately constant. Thus, according to Gallegos (1996) the temperature of the surface layer of the Caribbean Sea fol-

1 Laboratorio de Análisis Geoespacial. Instituto de Geografía. Universidad Nacional Autónoma de México. Ciudad Universitaria, México, D. F., 04510 México. raguirre@igg.unam.mx*

Recibido: 19 de marzo de 2014
Corregido: 26 de noviembre de 2014
Aceptado: 27 de enero de 2015

DOI: http://dx.doi.org/10.15359/revmar.7.1.

lows closely the annual cycle in terms of the heat-budget equation. On the other hand, although surface salinity may vary as a consequence of precipitation, evaporation, river discharge, upwelling, and currents, the core of the North Atlantic Subtropical Subsuperficial Water (NASSW) is a convenient and reliable indicator of persistent upper level circulation. Non-conservative properties, such as fluorescence, may vary as a function of the conservative ones, but usually around the core of the NASSW (e. g. Taguchi *et al.* 1988; Shcherbina *et al*. 2008). Based on these facts, it is feasible to consider our measurements are representative of the upper mixed layer of the Caribbean waters.

According to Gallegos (1996) and Mooers and Maul (1998), the water column in the Caribbean Sea on average can be described as a four-layer system: a warm and relatively fresh surface mixed layer (< 100-m), a relatively warm and salty subsurface layer centered around 200 m, a relatively cold and fresh intermediate layer centered about 700 m, and a nearly homogeneous deep layer below 2000 m. Sheng and Tang (2003) quantified horizontal variations of monthly mean hydrography in the Western Caribbean Sea and found that horizontal variations of the monthly mean temperature in the top 100 m are small in February and August, although the monthly mean salinity show relatively large horizontal variations in the surface mixed layer, associated with river discharges. The monthly mean temperature and salinity in the subsurface and intermediate layers between 100 and 1000 m have relatively large horizontal variations. In the deep layer greater than 1500 m, the monthly mean temperature and salinity are horizontally nearly homogeneous.

On the other hand, chlorophyll fluorescence has been widely utilized as a mean for a rapid assessment of the distribution and biomass of oceanic phytoplankton and for estimating the rates of primary production (Kiefer *et al*. 1989; Chamberlain *et al.* 1990; Signoret *et al.* 2006). Additionally, solar-stimulated natural fluorescence has been used to estimate primary productivity by a number of authors (*e.g.*, Valdez-Holguín *et al.* 1995; García-Mendoza & Maske, 1996; Stegmann & Lewis, 1997; Aguirre-Gómez, 2002; Winter *et al.* 2002; Morrison, 2003). With the advent of high sensitive instruments, the analysis of fluorescence for vertical profiles has been significantly improved (Chang & Dickey, 2001; Prairie *et al*. 2011). Nonetheless, to our knowledge, little attention has been paid to the fluorescence characteristics of the Caribbean region (e. g. Taguchi *et al.* 1988). Hence, the aim of this paper is to examine the characteristics of *in vivo* chlorophyll fluorescence of the Caribbean Sea supported with hydrographic ancillary data.

Physical characteristics of study area. Northeast trade winds are the major source of energy for currents in the Caribbean Sea, blowing almost constantly over the region. The principal surface water masses entering the zone are the flows of the North Brazilian Current (NBC) and the North Equatorial Current (NEC). The NBC passes around Trinidad, turning west along the continental slope into the southern Caribbean. However, there is a seasonal switch in the amount of NBC water entering the region in this way. During springtime (February to May) a broad shallow flow (150-200 km) from the NBC, importantly modified by Amazon and Orinoco waters, enters the region between Trinidad and Barbados (Ffield, 2005). This water type is brackish, turbid, and has relatively high chlorophyll content. The rest of the year, a large amount of this water is diverted eastwards, thus the water entering the Caribbean between Trinidad and Barbados is mainly of NEC origin. This water type has alternatively a high clarity and a little vertical structure in the upper 100 m (Borstad, 1982). NEC water also passes into the southeast Caribbean through the passages on the Lesser Antilles Arc where it amounts nearly half of the total influx (Roemmich, 1981; Kinder, 1983), and into the northeast Caribbean. The North Equatorial Current generates a clockwise gyre, which is driven by the northeast trade winds. This current flows to the west and is joined from the south by that part of the South Equatorial Current that has turned across the equator into the North Atlantic. In its passage through the Caribbean the flow is driven by the east winds in this region and the water piles up in the Gulf of Mexico. The seasonal mixed layer depth in the Caribbean Sea deepens in winter down to 100 m around Trinidad but only to about 60-70 m along the coast in the Caribbean Current Jet. In summer the mixed layer depth shoals about 50 m deep in the east and slopes upwards to about 30 m near the American coastline.

The Caribbean Sea is considered an oligotrophic region. This fact can be supported in terms of its efficiency of light utilization. Morel (1978) reported a spatial efficiency ε_A (ratio of surface photosynthetic rate by the total photosynthetically active radiation) in the interval of 0.02-0.07% for the Caribbean Sea, which can be interpreted as a relatively low amount of phytoplankton within the euphotic zone. Thus, a deep oligotrophic profile is characteristic of the area with chlorophyll maxima occurring within the pycnocline and above the nitracline (Hobson & Lorenzen, 1972). When the pycnocline is deeper than 100 m, the subsurface chlorophyll maximum is found to be extremely weak.

MATERIALS AND METHODS

This study was carried out in the summer of 2001. Even though it has been over a decade since the oceanographic campaign, the information gathered is still valid. Hydrographic and fluorescence measurements were carried out down to 200 meters which corresponds to the (NASSW) (Gunn &Watts, 1982).

Hydrographic, meteorological and fluorescence measurements were performed over the Caribbean Sea in the oceanographic/meteorological cruise ECAC-3 (short for: *Experimento Climático en las Albercas de Agua Caliente de las Américas*), onboard the Justo Sierra RV (University of Mexico, UNAM) during the summer of 2001 (July 6 to 26). Oceanic observations were focused on conductivity, temperature and depth casts made four or more times daily for temperature, salinity (measured using the Practical Salinity Scale), and pressure (CTD Neil Brown Mark-III), density and dissolved oxygen (DO) depth profiles, and fluorescence measurements. The cruise track had three phases: an outbound leg, the main survey, and an inbound leg. The outbound leg (from Tuxpan to the Yucatan Channel) was used for testing and training purposes. The cruise track for the main survey was determined by turning points that define the nine cruise legs as shown in Table 1. The inbound leg (from the Yucatan Channel to Tuxpan) was used for data processing and analysis, and database mergers. In particular, fluorescence measurements were carried out at 31 sampling stations located along the six cruise legs covering a great extension of the Caribbean Sea (Fig.1).

Fluorescence measurements. Vertical profiles of chlorophyll *a* fluorescence were recorded using the signal at 685 nm, with a WETStar Miniature Fluorometer (Wet Labs, Inc.). It is a small, lightweight instrument with an active sensor that allows the user to monitor chlorophyll concentrations by directly measuring the amount of fluorescence emission from a given sample of water. The sample media is pumped through a quartz tube mounted along the axis of the instrument. Chlorophyll, when excited by energy of short wavelength of the visible spectrum, is capable of absorbing it and re-emitting a small portion of this light as fluorescence at longer wavelengths. Particularly, blue light excitation (460 nm) is absorbed by phytoplankton, which contains chlorophyll. This energy is re-emitted as red

Table 1. Geographical location of the nine transects sampled during the cruise
Cuadro 1. Posición geográfica de los nueve transectos muestreados durante el crucero

Legs	**Initial location N,W**	**Final location N,W**	**Elapsed time**
I	21° 00’; 86° 42’	17° 30’; 78° 00’	0720 on 11 JUL to 1210 on 14 JUL
II	17° 30’; 78° 00’	15° 00’; 80° 42’	1210 on 14 JUL to 1730 on 15 JUL
III	15° 00’; 80° 42’	13° 00’; 79° 48’	1730 on 15 JUL to 1525 on 16 JUL
IV	13° 00’; 79° 48’	15° 00’; 79° 30’	1525 on 16 JUL to 0755 on 17 JUL
V	15° 00’; 79° 30’	13° 00’; 79° 00’	0755 on 17 JUL to 0230 on 18 JUL
VI	13° 00’; 79° 06’	13° 36’; 78° 42’	0230 on 18 JUL to 1210 on 18 JUL
VII	15° 42’; 80° 36’	19° 12’; 86° 24’	1420 on 19 JUL to 1640 on 21 JUL
VIII	19° 12’; 86° 30’	21° 12’; 81° 60’	1640 on 21 JUL to 0745 on 23 JUL
IX	21° 12’; 81° 06’	21° 36’; 85° 36’	0745 on 23 JUL to 0800 on 24 JUL

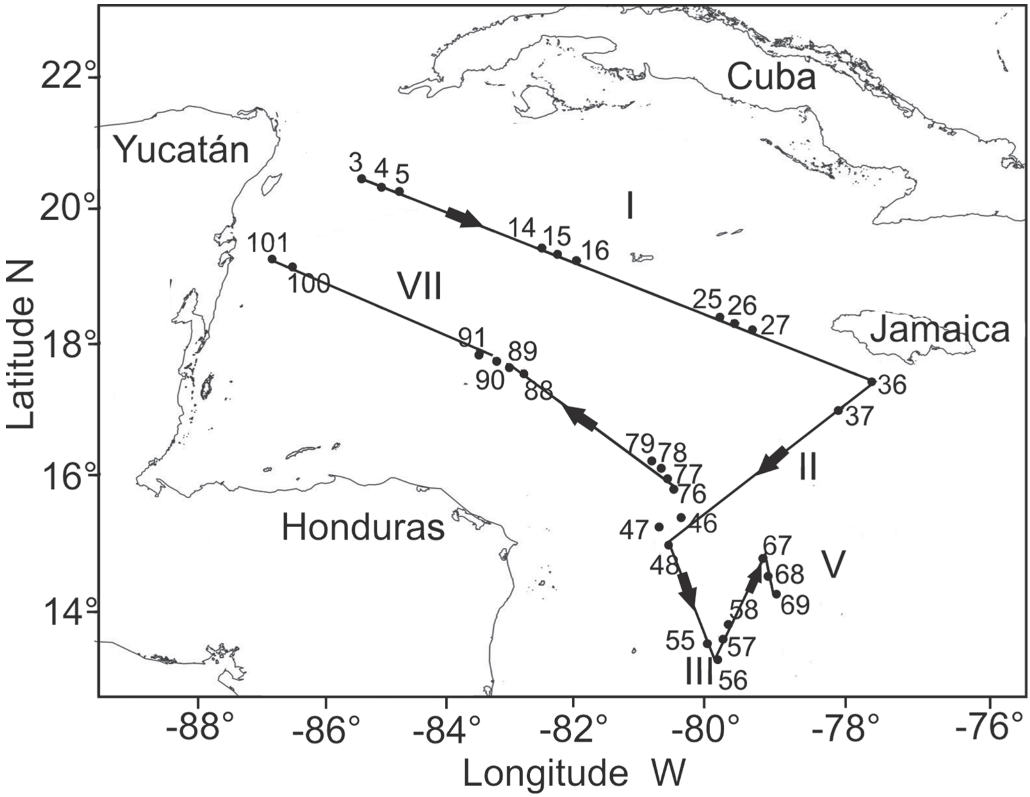

Fig. 1. ECAC-3 cruise track from July 6 - 26, 2001
Fig. 1. Trayecto del crucero ECAC-3 del 6 al 26 de julio de 2001

light at 690 nm. Scattered blue light is blocked by a red interference filter. The red fluoresced light passes through an interference filter and is detected by a photodiode, which, in turn passes the analog signal as a DC output voltage that can be measured and recorded. The sensor was coupled to one of the CTD connectors. This configuration guaranteed a constant flow when lowering the instrument steadily at 1.0 m per second, as well as the possibility of merging fluorescence information with CTD data. Thus, depth correlations were made. The instrument was calibrated prior to deploying it by using similar water as the one expected to be encountered *in situ* and by taking a chlorophyll sample close to the mooring. The instrument was deployed down to a depth of 200 m in order to cover the subsurface maximum of chlorophyll, which, for tropical waters has been found within this interval (Furuya, 1990; Bidigare *et al*. 1993).

Chlorophyll concentration was obtained through a linear relationship as follows:

$$[Chl] = (V_{sample} - V_{blank}) * \text{Scale factor} \quad (1)$$

Where,

[Chl] = Concentration of chlorophyll sample of interest (mg m^{-3})

V_{sample}= voltage output when measuring a sample of interest (VDC)

V_{blank}= measured signal for a sea water blank (VDC), which, in our case was 0.077

Scale factor = multiplier calculated by using the known chlorophyll concentration and its voltage response. The scale factor was calculated at 0.1629.

The chlorophyll *a* concentration was calculated by adjusting fluorescence vertical profiles as Gaussian shaped curves. A Gaussian profile was used to describe the vertical distribution of chlorophyll biomass in the ocean (Lewis *et al.* 1983). A shifted Gaussian model was later introduced considering a constant background superimposed on a Gaussian profile (Morel & Berthon, 1989; Sathyendranath & Platt, 1989; Gordon, 1992). The shifted Gaussian model suitably describes the vertical distribution of chlorophyll at a wide range of locations in the ocean. This model can be expressed as follows:

$$B(z) = B_0 + \frac{h}{\sigma\sqrt{2\pi}} \exp\left(-\frac{(z - z_m)^2}{2\sigma^2}\right) \quad (2)$$

where B(z) is chlorophyll biomass as a function of depth, z (positive downwards); B_0 is the background concentration on which a Gaussian curve whose peak is centered at depth z_m is superimposed; σ and h are Gaussian parameters for the width of the peak and amplitude of the chlorophyll maximum, respectively. In this calculation the specific attenuation coefficient for biomass k_c and the attenuation coefficient for water k_u are implicitly considered. Formally, biomass must include both photosynthetically active biomass B(z) and phaeopigments, which also contributes to light attenuation C(z). Nonetheless, in the open ocean, the contribution of phaeopigments to C(z) is negligible (Longhurst *et al.* 1995). Hence, B(z) can be used to represent both quantities and compute the diffuse, vertical attenuation coefficient from B(z) as described by Sathyendranath & Platt (1988). Consequently, the depth-averaged chlorophyll biomass concentration (C) in a layer can be calculated using the following equation (Platt *et al.* 1988).

$$C(z) = C_0 + \frac{h}{\sigma\sqrt{2\pi}} \exp\left[-\frac{(z - z_m)^2}{2\sigma^2}\right] \quad (3)$$

Platt *et al.* (1994) have shown that, in a multi-component medium, the average attenuation coefficient for a layer is the sum of the average attenuation coefficient for the individual components. As a result, the background biomass can be treated separately from the superimposed Gaussian component and from the attenuation due to seawater itself or any other component either dissolved or suspended.

RESULTS

Meteorological conditions during the cruise were rather stable except for two days of adverse weather at the end of July of 2001. Table 2 shows the meteorological information gathered at the

Justo Sierra RV during the expedition. Mean values of these parameters indicate the stability of weather conditions. Thus, wind vectors had a mean magnitude of 6.37 (3.01) m s^{-1} at 138.42 (64.04) degrees and the remaining of meteorological parameters had a lesser variability: mean relative humidity 80.48% (4.13); mean barometric pressure 1010.7 (1.59); and air temperature 29.16 (0.85).

Hydrographic characteristics. Figure 2 shows the temperature profile for all of the sampled stations in the 0-200 m interval. There is an upper mixed layer of about 50 m with a temperature ranging between 28 and 30°C. It is followed by a slight thermocline localized between 50 to 100 m deep. From this point on temperature decreases down to 20°C at about a depth of 200 m. Salinity profiles are shown in Figure 3. Here the upper mixed layer of 50 m has a salinity of 36.1 PSU on average. A moderate halocline is seen between 50-100 m and from this point downwards salinity increases up to 37.0 at around a depth of 150 m. Caribbean water masses are represented in the T-S diagram shown in Figure 4. The upper mixed layer (0-50 m) is fully controlled by the North

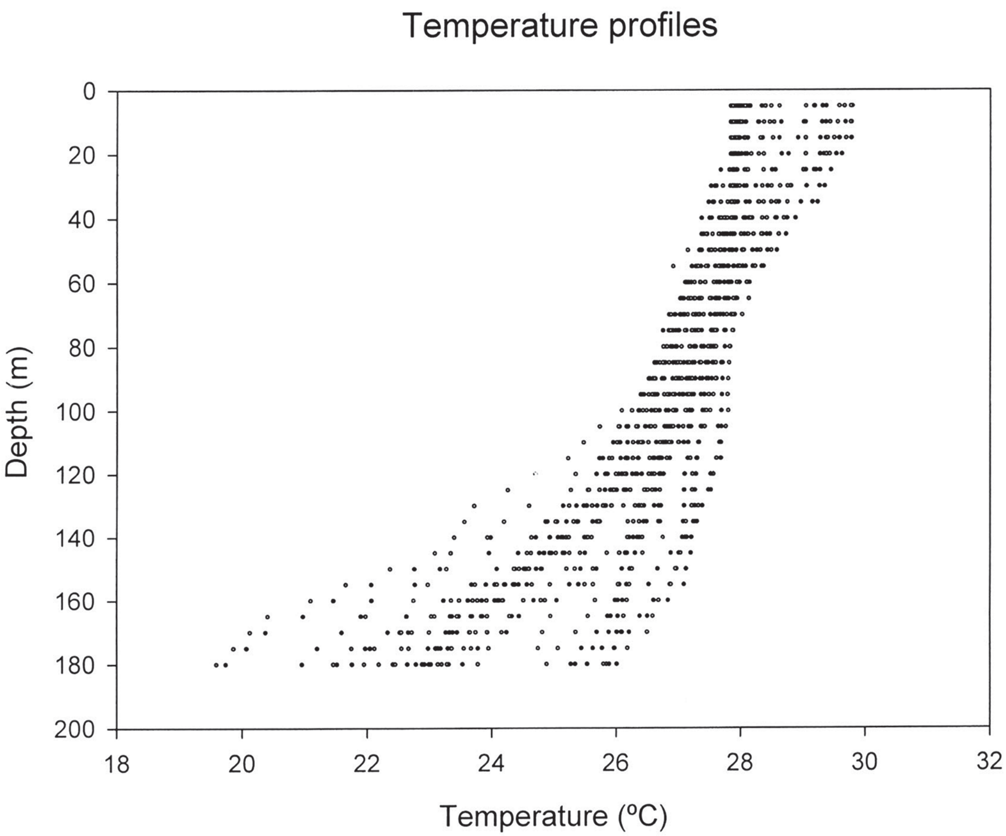

Fig. 2. Temperature profiles for all sampling stations from 0 to 200 m
Fig. 2. Perfiles de temperatura de todas las estaciones de muestreo de 0 a 200 m

Table 2. Meteorological parameters measured at the Justo Sierra RV: Latitude (Lat), Longitude (Lon), Wind direction (d), Wind speed (r), relative humidity (R.H.), Air Temperature (A.T.), Barometric Pressure (B.P.), time of measurements and date
Cuadro 2. Parámetros meteorológicos medidos en el buque oceanográfico Justo Sierra: Latitud (Lat), Longitud (Lon), Dirección del viento (d), Rapidez del viento (r), Humedad relativa (H.R.), Temperatura del aire (A.T.), Presión barométrica (B.P.), Hora de medición y fecha

S.S	Lat (N)	Lon (W)	W(d) ($m\ s^{-1}$)	W(r) ($m\ s^{-1}$)	R.H. (%)	A.T. (ºC)	B.P. (mb)	Time	Date (ddmmyy)
003	20° 21’	85° 37’	199	6.32	76	28.5	1012	08:58	110701
004	20° 16’	85° 22’	134	4.42	72	29.4	1012	12:45	110701
005	20° 10’	85° 07’	125	3.7	72	29.4	1011	14:20	110701
014	19° 29’	83° 10’	155	8.33	76	29.0	1013	08:15	120701
015	19° 22’	82° 53’	155	5.40	78	29.2	1014	10:52	120701
016	19° 17’	82° 38’	147	3.44	77	29.3	1013	13:10	120701
025	18° 27’	80° 26’	339	10.84	82	28.5	1013	09:15	130701
026	18° 21’	80° 11’	157	6.48	82	28.9	1013	13:25	130701
027	18° 16’	79° 56’	101	2.98	81	28.7	1012	13:25	130701
036	17° 19’	78° 11’	120	7.25	79	28.4	1010	09:20	140701
037	16° 44’	78° 36’	083	5.25	78	28.3	1009	13:30	140701
046	15° 07’	80° 24’	157	6.68	84	28.1	1009	09:15	150701
047	15° 00’	80° 40’	062	6.94	84	28.1	1009	12:40	150701
048	14° 44’	80° 37’	117	6.17	84	28.2	1008	15:00	150701
055	13° 06’	79° 57’	195	3.91	87	28.3	1010	08:16	160701
056	13° 00’	79° 49’	130	6.01	87	28.3	1010	10:00	160701
057	13° 15’	79° 47’	333	7.30	87	28.3	1010	12:10	160701
058	13° 29’	79° 44’	125	6.06	87	28.4	1009	14:30	160701
067	14° 15’	79° 20’	154	12.39	84	28.8	1010	10:00	170701
068	14° 01’	79° 17’	159	11.51	84	28.9	1009	11:50	170701
069	13° 46’	79° 14’	103	11.41	82	29.3	1008	14:17	170701
076	15° 44’	80° 38’	139	12.13	79	29.5	1010	09:40	190701
077	16° 00’	80° 41’	106	8.02	81	29.6	1011	11:15	190701
078	16° 15’	80° 49’	125	8.02	82	29.8	1010	13:30	190701
079	16° 22’	80° 53’	093	5.96	81	30.0	1010	14:30	190701
088	17° 35’	83° 23’	015	4.21	80	29.9	1012	09:30	200701
089	17° 41’	83° 37’	083	2.98	81	29.9	1012	10:57	200701
090	17° 47’	83° 52’	107	2.36	79	30.2	1012	13:34	200701
091	17° 54’	84° 06’	117	2.42	77	31.0	1010	15:39	200701
100	19° 02’	86° 08’	128	2.57	75	31.1	1010	08:30	210701
101	19° 09’	86° 20’	128	2.11	77	30.6	1010	09:55	210701

Equatorial Current (NEC) which is warm (25-30°C) and has relatively low salinity ranging between 36 and 36.5 PSU. Below the upper mixed layer (50-200 m) the dominant mass water is that of the NASSW, which has, according to Gunn & Watts (1982), a temperature range between 21-23°C and a salinity range between 36.6-37 PSU. NASSW is characterized by having the salinity maximum of all Caribbean waters, at an average depth of 150 m.

In vivo chlorophyll fluorescence. *In vivo* fluorescence in the water column showed a Subsurface Chlorophyll Maximum (SCM) at a mean depth of 107 m (Fig. 5). The spatial structure of the fluorescence of each transept is showed in Figure 6. Darker gray tones show the highest values of fluorescence. It is apparent from it that the SCM was nearly located at the same depth in all of them; therefore, a homogeneous distribution of chlorophyll *a* in the western Caribbean Sea can be inferred. The mean value of chlorophyll concentration varying around a depth of 107 m was 0.502 mg m^{-3}, (mean fluorescence value of 3.5V) according to equation 1. It must be clarified that transepts were either meridional or zonal. Fluorescence profiles were

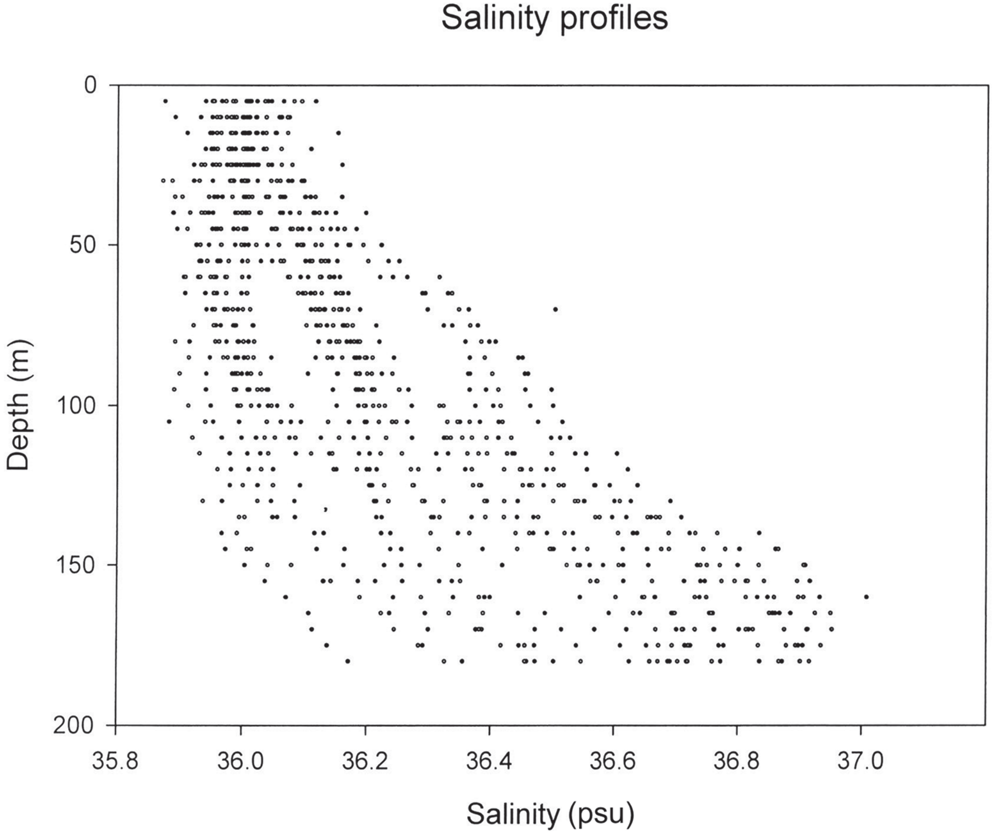

Fig. 3. Salinity profiles for all sampling stations from 0 to 200 m
Fig. 3. Perfiles de salinidad de todas las estaciones de muestreo de 0 a 200 m

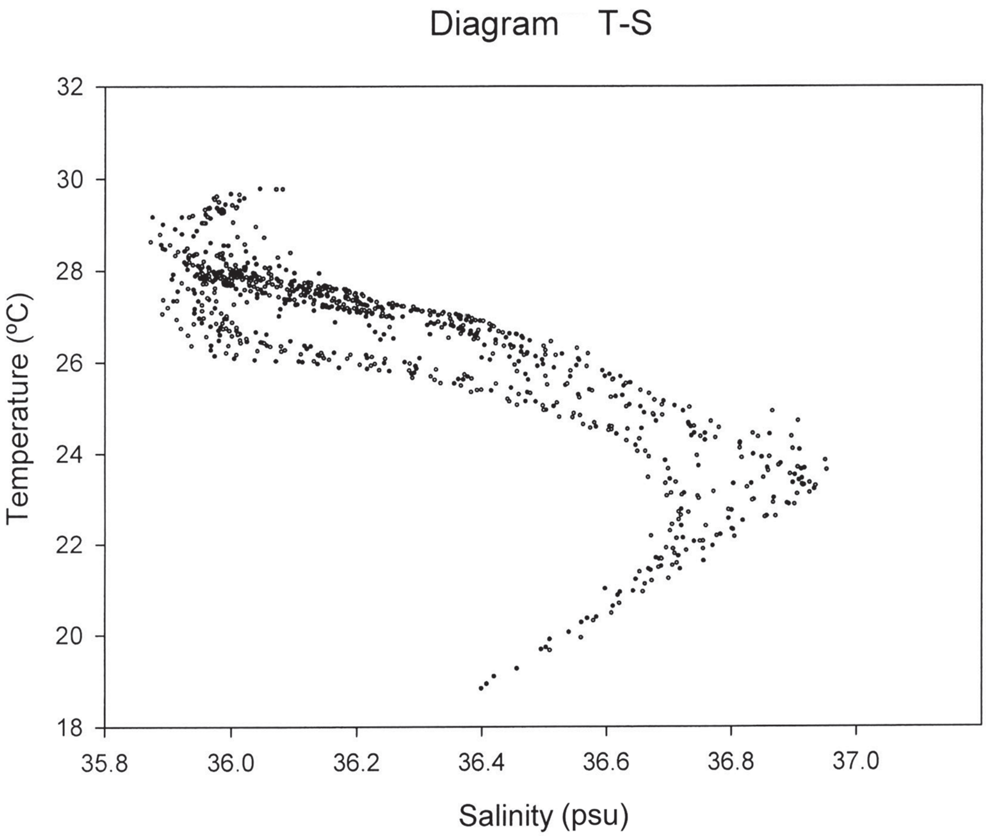

Fig. 4. T-S Diagram created with CTD data during ECAC-3 cruise for all sampling stations from 0 to 200 m depth
Fig. 4. Diagrama T-S creado con datos del CTD durante el crucero ECAC-3 para todas las estaciones de muestreo de 0 a 200 m

adjusted to shifted Gaussian-shaped curves according to Platt *et al.* (1994). The statistical parameters of equation 2 are shown in Table 3.

Based on Platt *et al.* (1988), the averaged chlorophyll concentration for all of the stations was 0.362 (σ=0.02) mg m^{-3} from the surface to a depth of 200 m. The chlorophyll concentration varied from 0.33 to a maximum of 0.40 mg m^{-3}. This range of values reinforces the rather typical oligotrophic waters of Caribbean Sea.

Figure 7 shows a temperature-fluorescence diagram. It is evident that the fluorescence maximum occurs at around 27°C, while, on the other hand, a salinity-fluorescence diagram suggests a binomial distribution between these two parameters (Fig. 8). However, from the T-S diagram (Fig. 4) it might be inferred that a salinity of around 36.3 PSU is coincident with a 27°C temperature. This temperature value is at about a depth of 107 m where the confluence of NEC and

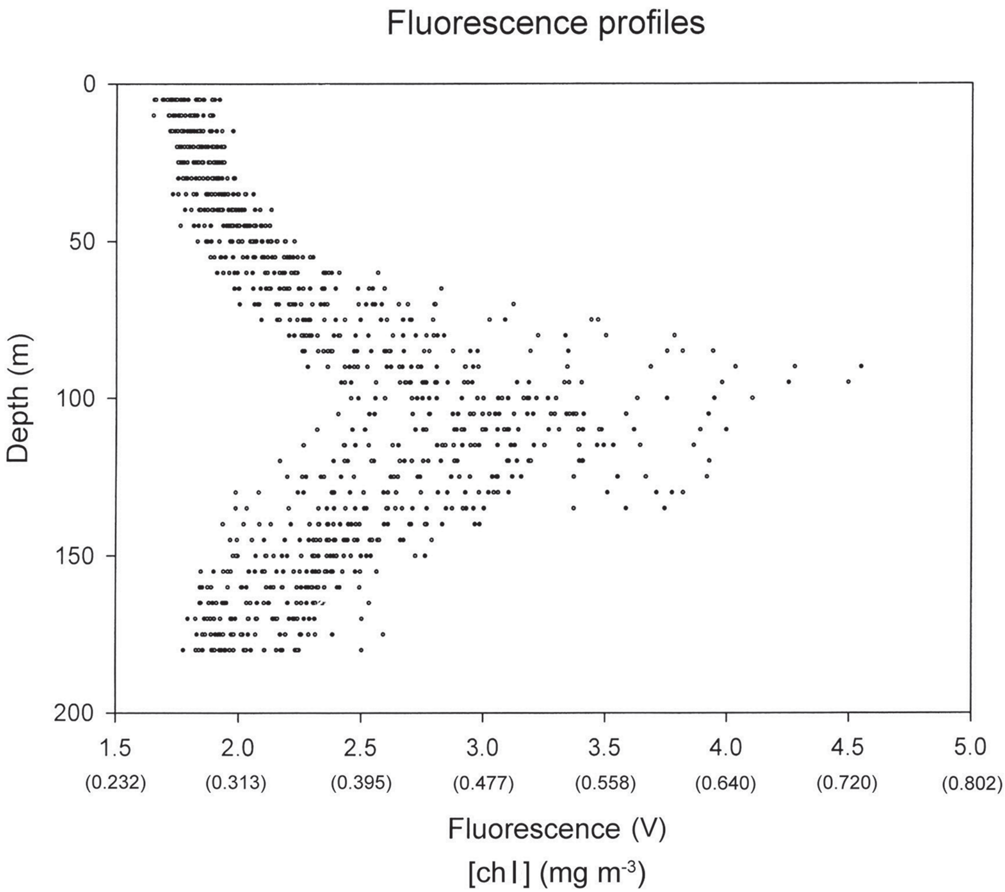

Fig. 5. Fluorescence profiles for all sampling stations from 0 to 200 m. The SCM is located at approximately a depth of 107 m

Fig. 5. Perfiles de fluorescencia para todas las estaciones de muestreo de 0 a 200 m. El Máximo Superficial de Clorofila se ubica alrededor de los 107 m de profundidad

NASSW takes place.

DISCUSSION

In tropical oceans, the sea surface temperature is much warmer than that of the deeper water. In the thermocline, the transition from warm water to cold water occurs rapidly. Above the thermocline, in the oceanic mixed layer, the water is fairly uniform in temperature and is approximately as warm as the sea surface (Ginis, 1995; Yablonsky & Ginis, 2013). Below the thermocline, the water is also nearly uniform in temperature but colder. The oceanic mixed layer in the Caribbean Sea is relatively thick, and the thermocline is deeper. This fact allows us to state that even though our data is relatively old, over time conditions at measured depths do not significantly change.

According to Farmer *et al.* (1993), during July the influx of NEC waters entering the Caribbean present little vertical structure in the upper 100 m, which

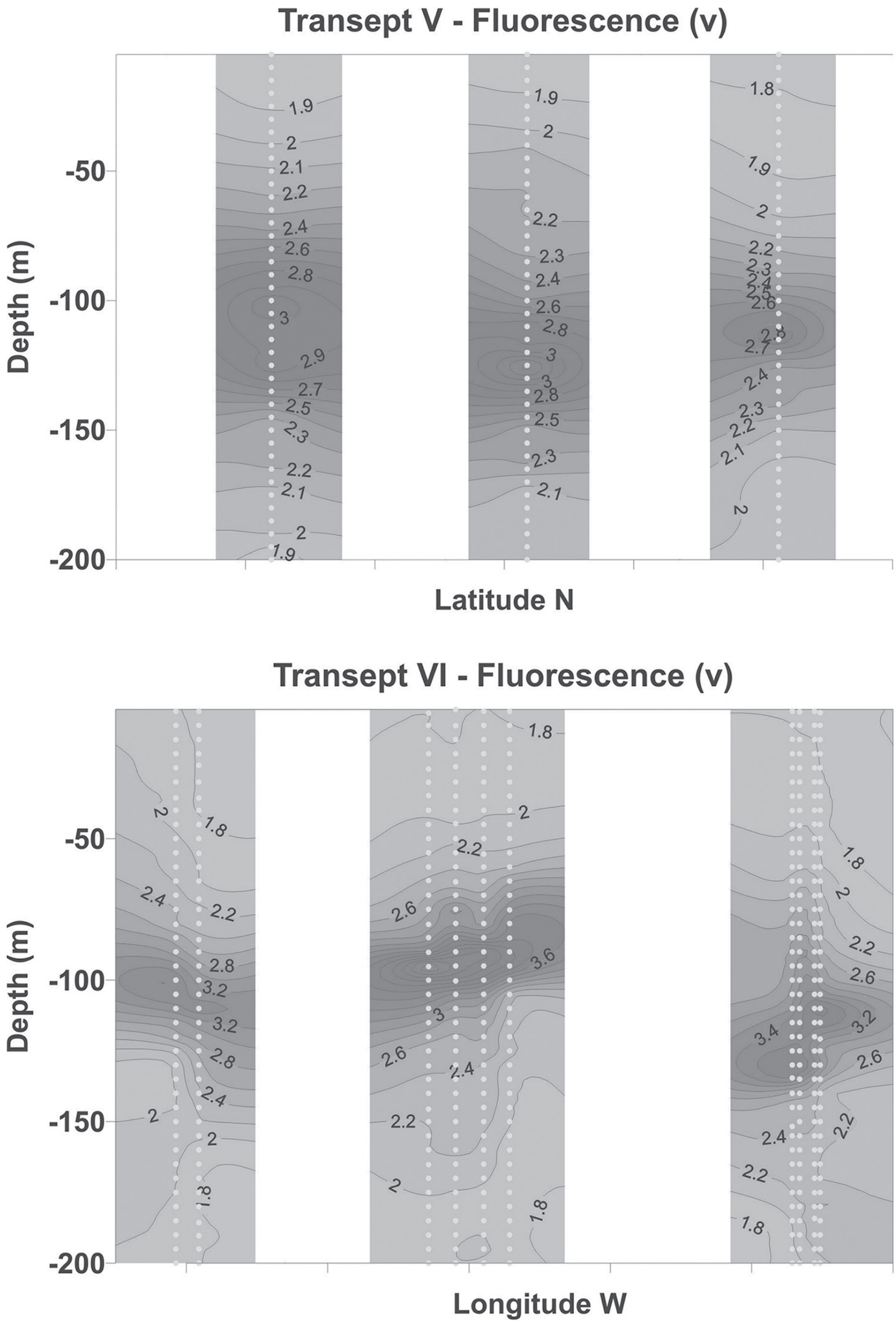

Fig. 6. Fluorescence horizontal spatial structure for transect from 0 to 200 m. The SCM is located at approximately a depth of 107 m

Fig. 6. Estructura especial horizontal de la fluorescencia de 0 a 200 m. El Máximo Superficial de Clorofila se ubica alrededor de los 107 m de profundidad

Table 3. Statistical parameters of Gaussian curves: σ (width of the curve); h (amplitude of the curve) and B_0 (background concentration) at the chlorophyll maximum
Cuadro 3. Parámetros estadísticos de las curvas Gaussianas: σ (ancho de la curva); h (amplitud de la curva) y B_0 (concentración de fondo) en el máximo de clorofila

	Depth	σ	h	B_0
mean	107.208	23.788	13.121	0.301
Standard deviation	11.649	8.725	3.911	0.017
Min	78.615	13.154	7.002	0.267
Max	130.106	42.401	21.527	0.331

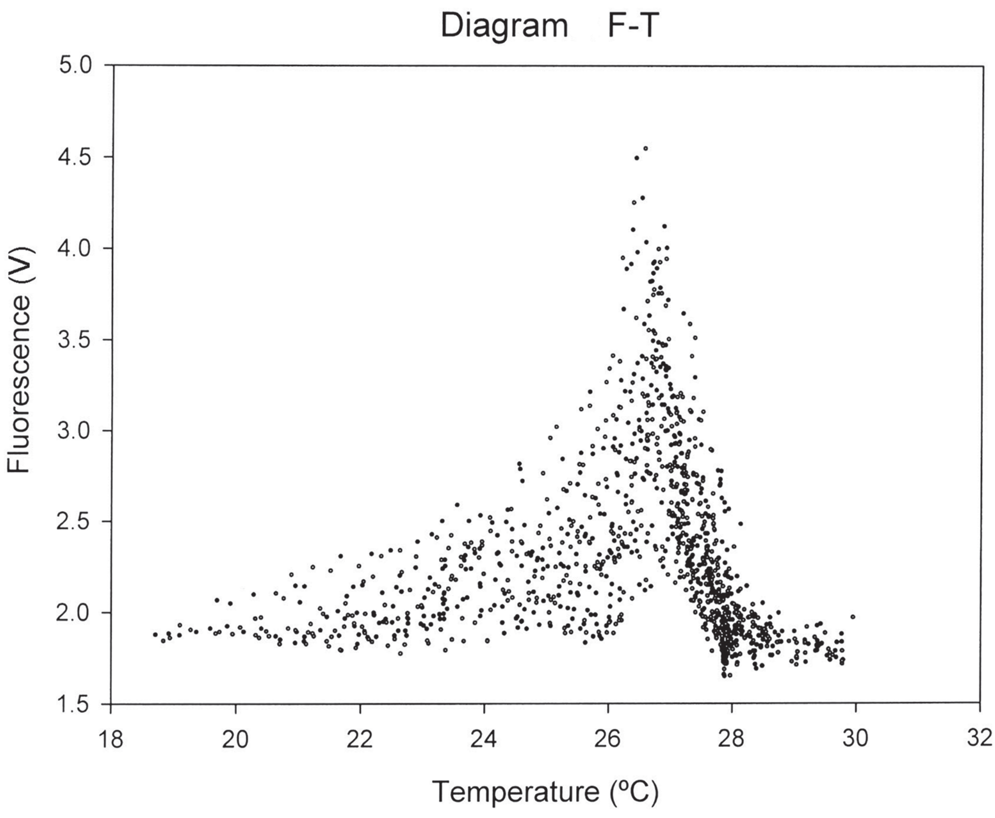

Fig. 7. F-T Diagram created with CTD data during ECAC-3 cruise for all sampling stations from depths of 0 to 200 m
Fig. 7. Diagrama F-T creado con datos del CTD durante el crucero ECAC-3 para todas las estaciones de muestreo de 0 a 200 m

is confirmed by the results of this research. Thus, fluorescence characteristics of the Caribbean Sea were measured with a high spectral resolution fluorometer. Fluorescence data shows typical profiles of tropical waters.

Thus, presence of chlorophyll can be reliably established from fluorescence measurements. This response is mainly due to the oligotrophic characteristics of the zone with deep chlorophyll maximum located at approximately 107 m. Shcherbina *et al*. (2008) collected chlorophyll a fluorescence data near the Belizean coast, among other bathymetric and hydrographic measurements, finding a deep chlorophyll maximum at approximately 80 m. Taguchi *et al.* (1988) found similar deep chlorophyll maxima in the eastern basin of the Caribbean Sea (98 ± 19 m), although higher values were found outside the Antilles arc. Additionally, it can be concluded that most of the Caribbean Sea waters show a similar optical characterization in Open Ocean. Coastal regions may present a different optical response due to river discharges or upwelling zones. Supporting this fact, a recent comprehensive analysis of the marine biodiversity of the Caribbean Sea was conducted

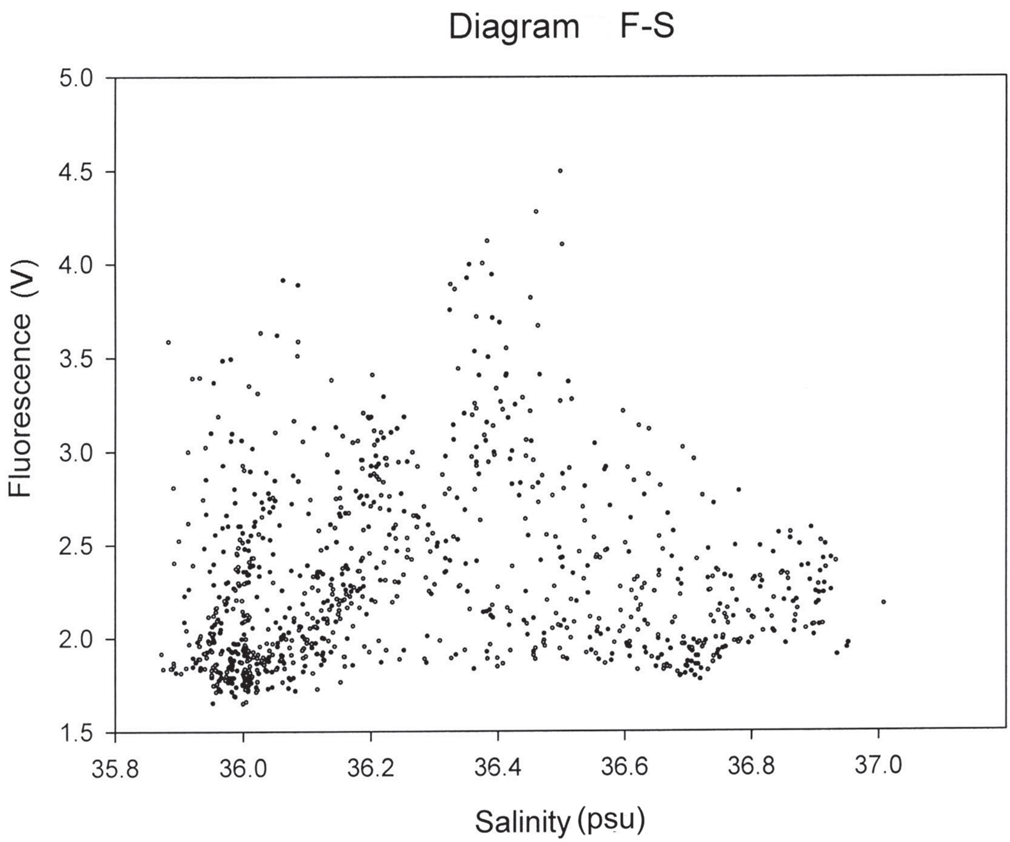

Fig. 8. F-S Diagram created with CTD data during ECAC-3 cruise for all sampling stations from depths of 0 to 200 m
Fig. 8. Diagrama F-S creado con datos del CTD durante el crucero ECAC-3 para todas las estaciones de muestreo de 0 a 200 m

by Miloslavich *et al.* (2010). Here, a higher coastal biodiversity than at oceanic sites was documented mainly due to river discharges.

Temperature profiles were fairly compact down to 100 m; from this point on data had the tendency to be relatively dispersed. This behavior allows us to identify a conspicuous peak relating fluorescence and temperature in an F-T diagram at approximately 27°C. On the other hand, salinity data shows a quite dispersed pattern, resulting in a rather diffused F-S diagram but depicting a bi-modal distribution with one peak at around 36 PSU and the other at about 36.4 PSU. Salinity and temperature profiles evidently agree with the results obtained by Sheng and Tang (2003). Nevertheless, the T-S diagram clearly discriminates the different water masses in the Western Caribbean Sea.

ACKNOWLEDGMENTS

We would like to thank Dr. A. Gallegos for his kind invitation to participate in the ECAC-3 cruise. Thanks to Dr. V. Magaña, coordinator of the project and the IAI for funding these campaigns and to Tania Fernández for all the support provided during the cruise, as well as the technicians of Institute of Geography for the drawings and the crew of Justo Sierra RV (UNAM).

BIBLIOGRAPHY

Aguirre-Gómez, R. (2002). Primary production in the southern Gulf of Mexico estimated from solar-stimulated natural fluorescence. *Hidrobiológica, 12*(1)*,* 21-28.

Bidigare, R. R., Ondrusek, M. E. & Brooks, J. M. (1993). Influence of the Orinoco River outflow on distributions of algal pigments in the Caribbean Sea. *J. Geophys. Res. Oceans, 98*(C2)*,* 2259-2269. http://dx.doi.org/10.1029/92JC02762

Borstad, G. A. (1982). The influence of the meandering Guiana Current and Amazon River discharge on surface salinity near Barbados. *J. Mar. Res.*, *40,* 421-434.

Chamberlain, W. S., Booth, C. R., Kieffer, D. A., Morrow, J. H. & Murphy, R. C. (1990). Evidence for a simple relationship between natural fluorescence, photosynthesis and chlorophyll in the sea. *Deep-Sea Res., 37*(6)*,* 951-973. http://dx.doi.org/10.1016/0198-0149(90)90105-5

Chang, G. C. & Dickey, T. D. (2001). Optical and physical variability on timescales from minutes to the seasonal cycle on the New England shelf: July 1996 to June 1997. *J. Geophys. Res-Oceans, 106*(C5), 9435-9453. http://dx.doi.org/10.1029/2000JC900069

Etter, P. C., Lamb, P. J. & Portis, D. H. (1987). Heat and freshwater budgets of the Caribbean Sea with revised estimates for the Central American Seas. *J. Phys. Oceanogr., 17*, 1232-1248. http://dx.doi.org/10.1175/1520-0485(1987)017<1232:HAFBOT>2.0.CO;2

Farmer, C. T., Moore, C. A., Zika, R. G. & Sikorski, R. J. (1993). Effects of low and high Orinoco river flow on the underwater light field of the eastern Caribbean Basin. *J. Geophys. Res-Oceans*, *98*(C2), 2279-2288. http://dx.doi.org/10.1029/92JC02764

Ffield, A. (2005). North Brazil current rings viewed by TRMM Microwave Imager SST and the influence of the Amazon plume. *Deep-Sea Res., (I), 52*(1), 137-160. http://dx.doi.org/10.1016/j.dsr.2004.05.013

Furuya, K. (1990). Subsurface chlorophyll maximum in the tropical and subtropical western Pacific Ocean: Vertical profiles of phytoplankton biomass and its relationship with chlorophyll *a* and particulate organic carbon. *Mar. Biol., 107*(3), 529-539.

Gallegos, A. (1996). Descriptive physical oceanography of the Caribbean Sea. In G. A. Maul (Ed.), *Small Islands: Marine Science and Sustainable Development*, *Coast. Estuar. Stud* (pp. 36-55). Washington D. C., EE.UU.: American Geophysical Union.

Gallegos, A. & Czitrom, S. (1997). Aspectos de la oceanografía física regional del Mar Caribe. En M. F. Lavin (Ed.), *Contribuciones a la Oceanografía Física en México, Monografía 3* (pp. 225-242). México, México, D. F.: Unión Geofísica Mexicana.

García-Mendoza, E. & Maske, H. (1996). The relationship of solar-stimulated natural fluorescence and primary productivity in Mexican Pacific waters. *Limnol. Oceanogr.*, *41*(8), 1697-1710.

Ginis, I. (1995). Ocean response to tropical cyclones. In R. Elsberry (Ed.), *Global Perspectives on Tropical Cyclones* (pp. 198-260). Geneva, Switzerland: World Meteorological Organization.

Gordon, A. L. (1967). Circulation of the Caribbean Sea. *J. Geophys. Res., 72*(24), 6207-6223. http://dx.doi.org/10.1029/JZ072i024p06207

Gordon, H. R. (1992). Diffuse reflectance of the ocean: Influence of non-uniform phytoplankton pigment profile. *Appl. Optics, 31*(12), 2116-2129. http://dx.doi.org/10.1364/AO.31.002116

Gunn, J. T. & Watts, D. R. (1982). On the currents and water masses north of the Antilles/Bahamas Arc. *J. Mar. Res., 40*(1), 1-18.

Hobson, L. A. & Lorenzen, C. J. (1972). Relationship of chlorophyll maxima to density structure in the Atlantic Ocean and Gulf of Mexico. *Deep Sea Res., 19*(4), 297-306. http://dx.doi.org/10.1016/0011-7471(72)90023-X

Kiefer, D. A., Chamberlin, W. S. & Booth, C. R. (1989). Natural fluorescence of chlorophyll a: Relationship to photosynthesis and chlorophyll concentration in the western South Pacific gyre. *Limnol. Oceanogr., 34*(5), 868-881. http://dx.doi.org/10.4319/lo.1989.34.5.0868

Kinder, T. H. (1983). Shallow currents in the Caribbean Sea and Gulf of Mexico as observed with satellite-tracked drifters. *Bull. Mar. Sci., 33*(2), 239-246.

Kinder, T. H., Heburn, G. W. & Green, A. W. (1985). Some aspects of the Caribbean circulation. *Mar. Geol., 68*(1), 25-52. http://dx.doi.org/10.1016/0025-3227(85)90004-0

Lewis, M. R., Cullen, J. J. & Platt, T. (1983). Phytoplankton and thermal structure in the upper ocean: Consequence of non-uniformity in chlorophyll profile. *J. Geophys. Res., 88*(C4), 2565-2570. http://dx.doi.org/10.1029/JC088iC04p02565

Longhurst, A., Sathyendranath, S., Platt, T. & Caverhill, C. (1995). An estimate of global primary production in the ocean from satellite radiometer data. *J. Plankton Res., 17*(6), 1245-1271. http://dx.doi.org/10.1093/plankt/17.6.1245

Miloslavich, P., Díaz, J. M., Klein, E., Alvarado, J. J., Díaz, C., Gobin, J. & Ortiz, M. (2010). Marine biodiversity in the Caribbean: Regional estimates and distribution patterns. *PLoS ONE*, *5*(8), e11916. doi:10.1371/journal.pone.0011916

Mooers, C. N. K. & Maul, G. A. (1998). Intra-Americas sea circulation, coastal segment (3,W). In A. Robinson & K. H. Brink (Eds.), *The Sea*, Vol. 11 (pp. 183-208). New York, EE.UU.: John Wiley and Sons.

Morel, A. (1978). Available, usable and stored radiant energy in relation to marine photosynthesis. *Deep-Sea Res., 25*(8), 673-688. http://dx.doi.org/10.1016/0146-6291(78)90623-9

Morel, A. & Berthon, J. F. (1989). Surface pigments, algal biomass profiles, and potential production of the euphotic layer: Relationships reinvestigated in view of remote-sensing applications. *Limnol. Oceanogr., 34*(8), 1545-1562. http://dx.doi.org/10.4319/lo.1989.34.8.1545

Morrison, J. R. (2003). In situ determination of the quantum yield of phytoplankton chlorophyll a fluorescence: A simple algorithm, observations, and a model. *Limnol. Oceanogr., 48*(2), 618-631. http://dx.doi.org/10.4319/lo.2003.48.2.0618

Müller-Karger, F. E., McClain, C. R., Fisher, T. R., Esaias, W. E. & Varela, R. (1989). Pigment distribution in the Caribbean Sea: Observations from space. *Prog. Oceanogr., 23*(1), 23-64. http://dx.doi.org/10.1016/0079-6611(89)90024-4

Platt, T., Sathyendranath, S., Caverhill, C. M. & Lewis, M. R. (1988). Ocean Primary Production and available light: further algorithms for remote sensing. *Deep Sea Res., 35*(6), 855-879. http://dx.doi.org/10.1016/0198-0149(88)90064-7

Platt, T., Sathyendranath, S., White III, G. N. & Ravidran, P. (1994). Attenuation of visible light by phytoplankton in a vertical structured ocean: solutions and applications. *J. Plankton Res., 16*(11), 1461-1487. http://dx.doi.org/10.1093/plankt/16.11.146

Prairie, J. C., Franks, P. J., Jaffe, J. S., Doubell, M. J. & Yamazaki, H. (2011). Physical and biological controls of vertical gradients in phytoplankton. *Limnol. Oceanogr. Fluid & Environ., 1*(1), 75-90. http://dx.doi.org/10.1215/21573698-1267403

Roemmich, D. (1981). Circulation of the Caribbean Sea: A well-resolved inverse problem. *J. Geophys. Res., 86*(C9), 7993-8005. http://dx.doi.org/10.1029/JC086iC09p07993

Sathyendranath, S. & Platt, T. (1988). The spectral irradiance field at the surface and in the interior of the ocean: A model for applications in oceanography and remote sensing. *J. Geophys. Res., 93*(C8), 9270-9280. http://dx.doi.org/10.1029/JC093iC08p09270

Sathyendranath, S. & Platt, T. (1989). Remote sensing of ocean chlorophyll: Consequence of non-uniform pigment profile. *Appl. Optics, 28*(3), 490-495. http://dx.doi.org/10.1364/AO.28.000490

Shcherbina, A. Y., Gawarkiewicz, G. G., Linder, C. A. & Thorrold, S. R. (2008). Mapping bathymetric and hydrographic features of Glover's Reef, Belize, with a REMUS autonomous underwater vehicle. *Limnol. Oceanogr.*, *53*(5, part 2), 2264-2272. http://dx.doi.org/10.4319/lo.2008.53.5_part_2.2264

Sheinbaum, J., Zavala, J. & Candela, J. (1997). Modelación numérica del Golfo de México y Mar Caribe. En M. F. Lavin (Ed.), *Contribuciones a la Oceanografía Física en México, Monografía 3* (pp. 243-264). México, México D. F.: Unión Geofísica Mexicana.

Sheng, J. & Tang, L. (2003). A numerical study of circulation in the

Western Caribbean Sea. *J. Phys. Oceanogr., 33*, 2049-2069. http://dx.doi.org/10.1175/1520-0485(2003)033%3C2049:ANSOCI%3E2.0.CO;2

Signoret, M., Monreal-Gómez, M. A., Aldeco, J. & Salas-de-León, D. A. (2006). Hydrography, oxygen saturation, suspended particulate matter, and chlorophyll-*a* fluorescence in an oceanic region under freshwater influence. *Estuar. Coast. Shelf Sci., 69*(1-2), 153-164. http://dx.doi.org/10.1016/j.ecss.2006.04.011

Stegmann, P. M. & Lewis, M. R. (1997). Shipboard measurements of phytoplankton production and solar-stimulated fluorescence rates in the Northwest Atlantic. *Cont. Shelf Res.*, *17*(7), 743-760. http://dx.doi.org/10.1016/S0278-4343(96)00063-5

Taguchi, S., DiTullio, G. R. & Laws, E. A. (1988). Physiological characteristics and production of mixed layer and chlorophyll maximum phytoplankton populations in the Caribbean Sea and western Atlantic Ocean. *Deep-Sea Res., 35*(8), 1363-1377. http://dx.doi.org/10.1016/0198-0149(88)90088-X

Valdez-Holguín, J. E., Gaxiola-Castro, G. & Cervantes-Duarte, R. (1995). Primary productivity in the Gulf of California, calculated from the relationship between superficial irradiance and chlorophyll in the euphotic zone. *Cienc. Mar., 21*(3), 311-329.

Winter, A., Rost, B., Hilbrecht, H. & Elbrächter, M. (2002). Vertical and horizontal distribution of coccolithophores in the Caribbean Sea. *Geo-Mar. Lett., 22*(3), 150-161. http://dx.doi.org/10.1007/s00367-002-0108-8

Yablonsky**,** R. M. & Ginis, I. (2013). Impact of a warm ocean Eddy's circulation on hurricane-induced sea surface cooling with implications for hurricane intensity. *Mon. Wea. Rev.,* 141, 997-1021. http://dx.doi.org/10.1175/MWR-D-12-00248.1